Virologica Sinica (2020) 35:43–51
https://doi.org/10.1007/s12250-019-00159-4

www.virosin.org
www.springer.com/12250

RESEARCH ARTICLE

Identification and Characterization of a Distinct Strain of Beak and Feather Disease Virus in Southeast China

Yanmei Ma[1] · Xiaoyong Chen[1] · Keyuan Chen[1] · Xiancheng Zeng[1] · Shili Yang[1] · Wei Chang[1] · Yao Tang[3] · Xiaoli Chen[3] · Song Wang[1] · Ji-Long Chen[1,2]

Received: 11 March 2019 / Accepted: 5 August 2019 / Published online: 24 September 2019

Abstract

Beak and feather disease virus (BFDV) is an infectious agent responsible for feather degeneration and beak deformation in birds. In March 2017, an epidemic of psittacine beak and feather disease (PBFD) struck a farm in Fuzhou in the Fujian Province of southeast China, resulting in the death of 51 parrots. In this study, the disease was diagnosed and the pathogen was identified by PCR and whole genome sequencing. A distinct BFDV strain was identified and named as the FZ strain. This BFDV strain caused severe disease symptoms and pathological changes characteristic of typical PBFD in parrots, for example, loss of feathers and deformities of the beak and claws, and severe pathological changes in multiple organs of the infected birds. Phylogenetic analysis showed that the FZ strain was more closely related to the strain circulating in New Caledonia than the strains previously reported in China. Nucleotide homology between the FZ strain and other 43 strains of BFDV ranged from 80.0% to 92.0%. Blind passage experiment showed that this strain had limited replication capability in SPF Chicken Embryos and DF-1 Cells. Furthermore, the capsid (*Cap*) gene of this FZ strain was cloned into the pGEX-4T-1 expression vector to prepare the polyclonal anti-Cap antibody. Western blotting analysis using the anti-Cap antibody further confirmed that the diseased parrots were infected with BFDV. In this study, a PBFD and its pathogen was identified for the first time in Fujian Province of China, suggesting that future surveillance of BFDV should be performed.

Keywords Beak and feather disease virus (BFDV) · Parrot · FZ strain · Capsid protein (Cap) · Phylogenetic analysis

Introduction

Psittacine beak and feather disease (PBFD) has emerged as a major threat to parrot populations in recent years (Fogell *et al.* 2016). The classical symptoms of PBFD include symmetrical loss of contour, tail and down feathers and, in some species, deformities of the beak and claws (Pass and Perry 1984; Jergens *et al.* 1988; Nagase *et al.* 2005; Mcorist *et al.* 1984). This disease is widely distributed, infectious and often fatal, affecting a number of different psittacine species, including Amazons, macaws, parakeets, cockatoos, budgerigars and lorikeets (Ritchie *et al.* 1989a; Woods and Latimer 2000). In addition, a high prevalence of beak and feather disease was found in non-psittacine birds (Sarker *et al.* 2015b; Sarker *et al.* 2016; Amery-Gale *et al.* 2017). To date, PBFD has been reported in approximately 40 countries around the world, including detection in wild and captive flocks (Fogell *et al.* 2016, 2018). However, this disease has rarely been reported in China, except for cases found in Qingdao and Beijing (Hsu *et al.* 2006; Zhuang *et al.* 2012; Guo *et al.* 2018). The lack of epidemiological investigation made it difficult to estimate the current epidemic situation of PBFD in China.

The causative agent of PBFD is beak and feather disease virus (BFDV), which belongs to the *Circovirus* in the

Yanmei Ma and Xiaoyong Chen have contributed equally to this work.

Electronic supplementary material The online version of this article (https://doi.org/10.1007/s12250-019-00159-4) contains supplementary material, which is available to authorized users.

✉ Ji-Long Chen
chenjl@im.ac.cn

[1] Fujian Agriculture and Forestry University, Fuzhou 350002, China

[2] CAS Key Laboratory of Pathogenic Microbiology and Immunology, Institute of Microbiology, Chinese Academy of Sciences (CAS), Beijing 100101, China

[3] Fuzhou Zoo, Fuzhou 350012, China

family *Circoviridae* (Ritchie *et al.* 1989b; Allan *et al.* 2010; Ignjatovic 2010). BFDV is one of the smallest known pathogenic viruses. The size of the viral particle ranges from 14 to 20 nm in diameter (Regnard *et al.* 2017). A recent study using electron and atomic force microscopy showed that the BFDV particle size were either 10 nm or 17 nm according to the two distinct assembly forms of Cap protein (Subir *et al.* 2016). Meanwhile, BFDV comprises an icosahedral and symmetric capsid and a single-stranded DNA genome. The genome of BFDV is approximately 2 kb in size and contains two major opening reading frames (ORFs) that encode two distinct proteins, capsid (Cap) protein and replication-associated (Rep) protein (De and de Kloet 2004). The N-terminus of the Cap protein harbors nuclear localization signals, and the Cap protein most likely binds to viral DNA via the DNA-binding region and transports the Rep protein to the nucleus (Finsterbusch *et al.* 2005; Heath *et al.* 2006). It has been shown that BFDV spreads through both horizontal and vertical transmission (Todd 2004). Therefore, it is difficult to eliminate BFDV from an infected farm.

Unlike other circoviruses such as porcine circovirus (PCV) and chicken anaemia virus (CAV), *in vitro* propagation of BFDV using specific pathogen free (SPF) embryonated chicken eggs is a challenge (Raidal *et al.* 1993; Bassami *et al.* 1998). Since there is no effective method for propagate of BFDV *in vitro*, the development of commercial BFDV vaccines is hindered. Previous studies showed that immunizing parrots with inactive BFDV present in the feathers of a chronically infected parrot protects themselves from BFDV infection (Raidal and Cross 1994; Sarker *et al.* 2015a). However, because of the lack of a reliable and safe method to inactivate BFDV *in vitro*, the use of BFDV-infected feathers or other tissues as antigens to immunize healthy birds is considered a risk. Bonne *et al.* (2009) verified that the recombinant BFDV Cap protein expressed using the baculovirus system produces BFDV-specific serum and prevents virus replication, suggesting that the recombinant BFDV Cap protein promotes adaptive immune response against BFDV in inoculated parrots.

Recently, a PBFD epidemic struck a farm in Fuzhou in the Fujian Province of China, causing the death of parrots including lorikeets, parakeets, and macaws. Most of the dead parrots were young parakeets (within 6 months old), which exhibited typical feather loss, beak blackening, and claw deformability. Here we analyzed the clinical features and pathological anatomy of diseased parrots, and characterized the associated BFDV genome. Furthermore, a polyclonal antibody against the BFDV Cap protein was generated. Using this antibody, the expression of the viral Cap protein was detected in the infected birds. These results provide a reliable basis for further investigation of the molecular epidemiology of BFDV in Fujian Province, southeast of China.

Materials and Methods

Sample Collection

There are about 220 juveniles to adult parrots on the farm. Excrements samples were collected from 87 diseased parrots displaying signs of clinical symptoms of suspected PBFD. Several organs, including liver, intestine, kidney, muscular stomach, spleen, and heart, were collected from 51 died parrots (lorikeets), and processed for virus detection and histopathological examination.

Polymerase Chain Reaction (PCR) and Quantitative Real-Time PCR (qPCR)

Total DNA of the samples was extracted using a Stool DNA Kit D4015 (Omega Bio-tek, Inc., Norcross, GA) according to the manufacturer's instructions. The DNA was measured by NanoDrop2000 spectrophotometer (Thermo Scientific, Willmington, DE, USA). The fragment of BFDV *C1* gene was amplified using gene-specific primers which were designed by Primer Premier 5.0. PCR primers for avian polyomavirus-VP1 (APV-VP1) were designed as described previously (Kou *et al.* 2008), and the PCR products were sequenced. A known cDNA of BFDV *C1* gene was used as template of the positive control, and the negative control is ddH_2O. The primers used in the study were listed in Supplementary Table S1. Genes under study were amplified by PCR, using Easy*Taq* DNA Polymerase (TransGen Biotech, Beijing, China), or qPCR, using TransStart Tip Green Real-Time PCR SuperMix (Promega, Madison, Wisconsin, USA.). The PCR cycling conditions consisted of an initial denaturation at 95 °C for 5 min, followed by 35 cycles of 95 °C for 30 s, 56 °C–58 °C for 30 s, and 72 °C for 30 s, and a final extension at 72 °C for 10 min. qPCR conditions consisted of an initial denaturation at 50 °C for 2 min and 95 °C for 10 min, 40 cycles of 95 °C for 15 s and 51 °C for 30 s, and a final elongation step of 1 min at 60 °C. The amplified DNA fragments were visualized by electrophoresis on a 1.0% agarose gel, and purified using an EasyPure Quick Gel Extraction Kit (TransGen Biotech, Beijing, China).

Animal tissue was extracted to prepare DNA and equal amounts of the DNA were used for qPCR that was performed under same condition. The relative DNA levels of BFDV *C1* gene were analyzed by the $2'\Delta\Delta$Ct method using housekeeping gene (β-actin) as an internal normalization and plotted as fold changes compared with the lowest levels represented by 1.

Phylogenetic Analysis

To construct phylogenetic trees and analyze the nucleotide homology between the FZ strain and other strains of BFDV, DNA sequences obtained in this study were compared with entries available in the GenBank nucleotide sequence database. Whole-genome, *Rep*, and *Cap* sequences of BFDV were aligned using ClustalW (www.clustal.org/) with MEGA v5.2. Phylogenetic and molecular evolutionary analyses were performed using MEGA v5.2, and phylogenetic trees were constructed using the neighbor-joining (NJ) method, with 1000 bootstrap replications.

Blind Passage in SPF Chicken Embryos and DF-1 Cells

For virus isolation, liver specimen was homogenized in physiological saline solution, subjected to three freeze–thaw times, and clarified by centrifugation at 16,200 $\times g$ for 15 min. The obtained supernatant was added into DF1 cells for days and was collected for the infection to the second-generation cell separation experiment, and the supernatant of the first to sixth generation cells was collected. Besides, the supernatant from live specimen was injected into 8-day-old SPF chicken embryos via the chorioallantois membrane and incubated at 37 °C for 4 days. Five serial passages were performed and the presence of BFDV was verified by PCR and DNA sequencing.

Construction of BFDV-Cap Expression Vector

Codon-optimized *Cap* gene sequence of the FZ strain of BFDV (GenBank accession number MH188863) was synthesized by GENEWIZ (GENEWIZ, Inc., South Plainfield, NJ). The synthesized *Cap* gene was cloned into pGEX-4T-1 to express the GST fusion proteins, as previously described (Yang *et al.* 2013; Feng *et al.* 2018). To confirm that the correct BFDV DNA was cloned into pGEX-4T-1, a single colony was cultured at 37 °C overnight, and plasmid DNA extracted from the cells using a QIAprep Spin Miniprep Kit (Qiagen, Hilden, Germany), according to the manufacturer's instructions, was sequenced at Fuzhou TSING KE Biological Technology Co., Ltd. using vector sequencing primers. The recombinant plasmid was transformed into *Escherichia coli* BL21 cells (TransGen Biotech, Beijing, China) to express the GST-Cap fusion protein.

Preparation of Polyclonal Anti-Cap Antibody

Overnight cultures of *E. coli* BL21 transformed with pGEX-4T-1-Cap and pGEX-4T-1 empty vector were used to inoculate fresh Luria-Bertani (LB) medium supplemented with ampicillin (100 mg/mL). Cultures were incubated until the optical density reached 0.6–1.0, and protein expression was induced by the addition of IPTG (0.5 mmol/L final concentration). After 6 h of induction, bacteria were harvested by centrifugation, resuspended in phosphate-buffered saline (PBS), and subsequently lysed by sonication on ice with six, 30 s pulses. The lysate was centrifuged at 12,000 $\times g$ for 15 min, and the supernatant and precipitate were tested using sodium dodecyl sulfate-denaturing polyacrylamide gel electrophoresis (SDS-PAGE), as previously described (Lee *et al.* 2002). The target bands were cut out from the gel at the corresponding size and placed in 50-mL centrifuge tubes. These bands were sealed with dry ice and sent to Beijing Pekerat Lab Rabbit Breeding Biotechnology Development Co., Ltd. for the preparation of polyclonal antibodies.

Western Blotting

Liver lysates of BFDV infected parrots and the control uninfected controls were separated by SDS-PAGE. After electrophoresis, proteins were transferred to nitrocellulose membranes and blocked with 5% (w/v) milk powder dissolved in Tris-buffered saline (TBS; pH7.4) at 24 °C–26 °C for 2 h. Membranes were incubated with the indicated primary antibodies overnight at 4 °C and washed with TBS followed by incubation with appropriate secondary antibodies at 24 °C–26 °C for 2 h before imaging with the ProteinSimple FluorChem M system, as previously described (Wang *et al.* 2018).

Results

Probable PBFD Epidemic was Found in a Farm in Fujian Province of China

Diseased and dead parrots were found in a farm in Fuzhou, Fujian Province, China in March 2017. A total of 87 diseased parrots were collected for the investigation of disease symptoms. Of these, 51 parrots showing pathological lesions died. The disease symptoms included feather loss and deformed beak (Supplementary Figure S1).

Furthermore, we examined pathological changes in various organs of the parrots. Compared with the tissues of healthy parrots, the liver of diseased parrots showed blurring of intercellular boundaries in some areas, punctate necrosis, and edema of the hepatic sinusoids (Fig. 1A, 1B). The intestine of diseased parrots showed villi necrosis, epithelial cell damaged, and the presence of a large number of inflammatory cells in the basal layer. In addition, the crypt structure was significantly impaired, and epithelial

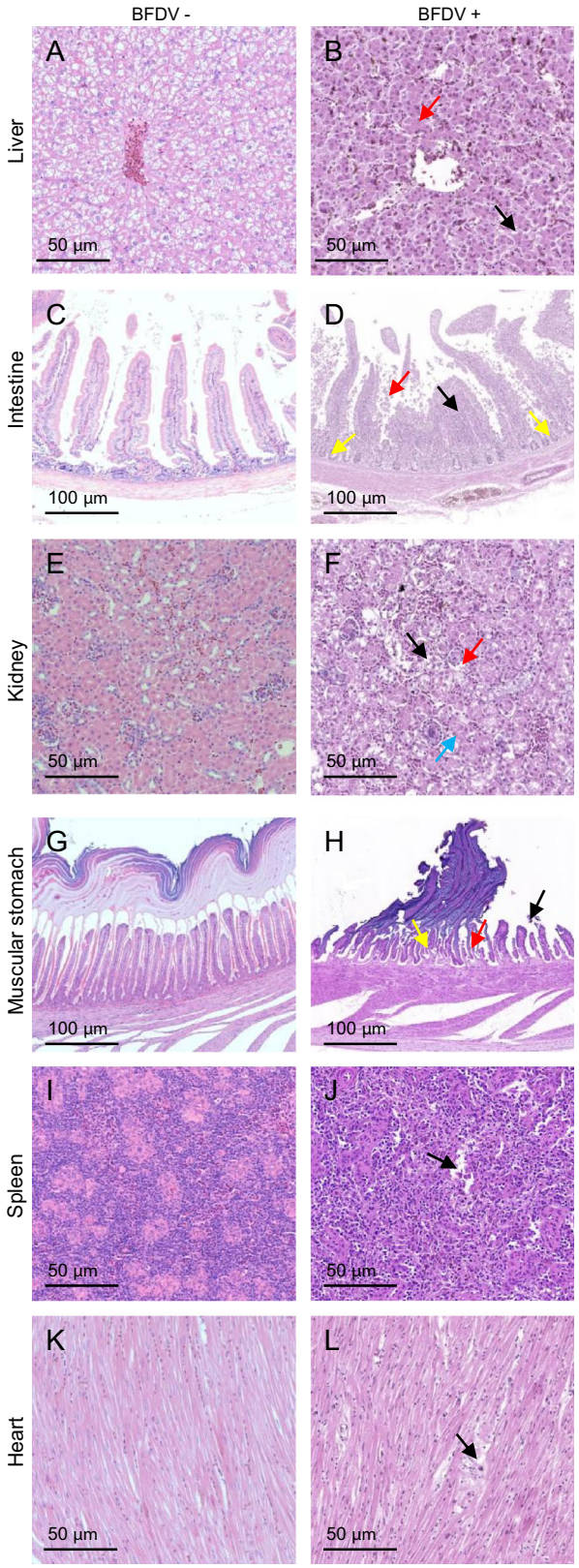

◀**Fig. 1** Histopathological analysis of organs of healthy and diseased parrots by hematoxylin and eosin staining. **A**, **B** Liver of a healthy parrot (**A**) and a diseased parrot (**B**); the diseased liver showed punctate necrosis (red arrow) and edema of hepatic sinusoids (black arrow). **C**, **D** Intestine of a healthy parrot (**C**) and a diseased parrot (**D**); the diseased intestine shows large number of inflammatory cells in the basal layer (black arrow), impaired crypt structure (yellow arrow), and epithelial cells necrosis (red arrow). **E**, **F** Kidney of a healthy parrot (**E**) and a diseased parrot (**F**); the diseased kidney showed an enlarged lumen of the glomerulus (red arrow), renal tubular epithelial cell edema (black arrow), and absent tubular structure (blue arrow). **G**, **H** Muscular stomach of a healthy parrot (**G**) and a diseased parrot (**H**); the infected muscular stomach showed ulcers in a localized area (black arrow), blocked gastric gland catheter with a narrow lumen (yellow arrow), and detached mucosal epithelium (red arrow). **I**, **J** Spleen of a healthy parrot (**I**) and a diseased parrot (**J**); the infected spleen shows the formation of a cavity because of cell necrosis in a localized area (black arrow). **K**, **L** Heart of a healthy parrot (**K**) and a diseased parrot (**L**); the diseased heart showed localized mild edema (black arrow).

cells were sparsely distributed (Fig. 1C, 1D). The kidney tissues of diseased parrots were characterized by a shrunken glomerular structure with an enlarged lumen and reduced number of capillaries, the shedding of renal tubular epithelial cells, and the absence of the typical tubular structure (Fig. 1E, 1F). Moreover, ulcers were observed in a localized area of the muscular stomach keratinized membrane. The gastric gland catheter in diseased parrots appeared to be blocked with a narrow lumen. The mucous layer in the mucosal region was atrophied and thinner in diseased parrots compared with healthy parrots (Fig. 1G, 1H). The spleen structure was slightly disordered with mild edema, and necrosis of cells was observed in a localized area, leading to the formation of a cavity (Fig. 1I, 1J). Myocardium fibers were neatly arranged in diseased parrots although mild edema was visible (Fig. 1K, 1L).

Identification of BFDV in Diseased Parrot

DNA was extracted from excrement samples from 87 diseased parrots and detectable in 45 excrement samples which were further examined for the presence of BFDV *C1* gene by PCR. BFDV *C1* gene was detected in 36 of the 45 samples (Fig. 2A), but all 45 samples were APV-negative. In addition, PCR results showed that BFDV was detectable in the heart, kidney, spleen, muscular stomach, lung, liver, and intestine of disease parrots (Fig. 2B). Relative expression levels of the BFDV *C1* gene in these organs were examined by qPCR. We found that the relative DNA levels of BFDV-C1 were higher in liver, intestine and lung than in spleen, heart, muscular stomach and kidney (Fig. 2C).

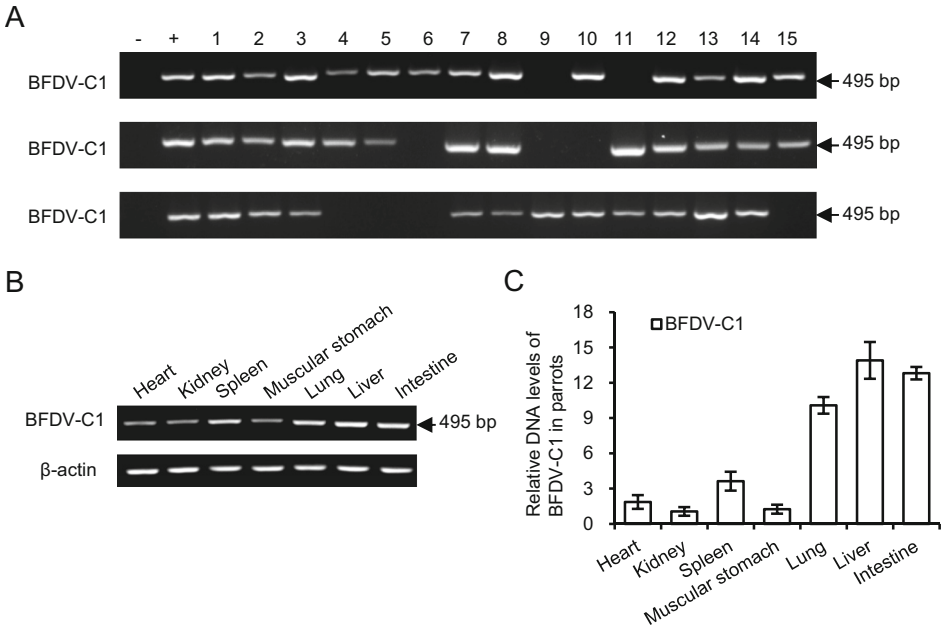

Fig. 2 BFDV *C1* gene detection in diseased parrots. Lane 1–15, represent DNA amplified from 45 parrots; M, DNA marker; −, negative control; +, positive control (**A**). PCR and qPCR methods were used to detect BFDV *C1* gene in various organs of the infected parrot, including heart, kidney, spleen, muscular stomach, lung, liver, and intestine (**B**, **C**).

Phylogenetic Analysis of the BFDV Genome

To further confirm the presence of BFDV in parrot feces and organs, the entire genome of BFDV was sequenced by Sangon Biotech [Sangon Biotech (Shanghai) Co., Ltd.]. BFDV genome isolated from three infected parrots was successfully sequenced and these sequences were identical. The whole genome sequence of BFDV amplified in this study was deposited in GenBank (accession number MH188863); this strain was named as FZ strain.

The FZ strain of BFDV has a DNA genome of 1,995 bp. Sequence comparisons using MEGA v5.2 showed that DNA sequences of the FZ strain were similar to whole-genome sequences of 43 previously reported BFDV strains available in GenBank, and their sequence similarity ranged from 80.0% to 92.0%. The genome of BFDV FZ strain contained two ORFs, *C1* and *V1*, encoding Cap and Rep proteins, respectively, and showed 80.5%–93.6% and 87.4%–95.8% nucleotide similarity with the corresponding domains of the published BFDV sequences. The FZ strain exhibited the typical genome structure of BFDV, as described previously (Niagro *et al.* 1998; Crowther *et al.* 2003), including the positions of ORFs and the presence of a stem-loop structure between the *Rep* and *Cap* genes.

To gain further understanding of the genetic relationship between BFDV FZ strain isolated in this study and 43 previously published BFDV genome sequences available in GenBank, we performed phylogenetic analysis of the whole BFDV genome. Phylogenetic trees were divided into five evolutionary branches, representing the association between BFDV strains at different times and geographical distributions. The FZ strain of BFDV clustered with BFDV strains from New Caledonia (Fig. 3A). Similar to the results of whole genome sequence analysis of the FZ strain, phylogenetic analysis showed that *Cap* and *Rep* genes were closely related to BFDV strains from New Caledonia (Fig. 3B, 3C).

Limited Replication of BFDV in SPF Chicken Embryos and DF-1 Cells

To verify whether BFDV could replicate *in vitro*, the BFDV *C1* gene was detected by PCR in allantoic fluid after five blindly passages but was undetectable after four passages in SPF chicken embryos allantoic cavity (Fig. 4A). To confirm this observation, DF-1 cells were inoculated with supernatant from BFDV-positive livers, and the virus was blindly passaged for six generations. The virus gene was detected in DF-1 cells after four passages but could not be detected in the fifth passage (Fig. 4B).

Expression of BFDV Cap Protein in Infected Parrots

A 759-bp fragment of the *Cap* coding sequence was amplified by PCR using a pair of gene-specific primers (Fig. 5A), and cloned into pGEX-4T-1 vector for the construction of pGEX-4T-1-Cap (Fig. 5B). Comparison between the protein products of pGEX-4T-1 and pGEX-4T-1-Cap revealed a band of approximately 50 kDa (Fig. 5C), indicating the expression of GST-Cap after induction by IPTG. Analysis of the solubility of GST-Cap revealed that most of the recombinant protein was present in inclusion bodies (Fig. 5D). Western blotting analysis

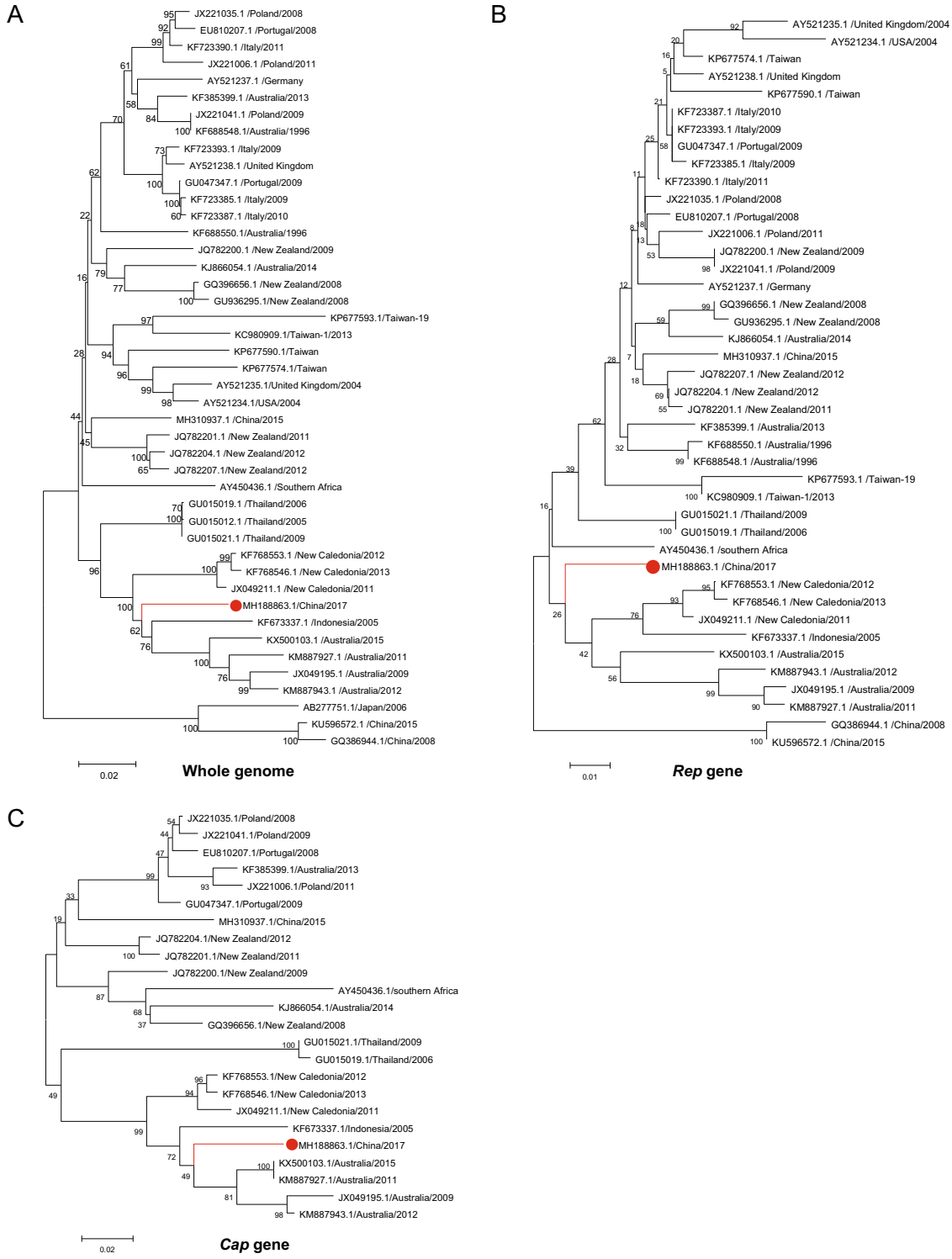

Fig. 3 Phylogenetic analysis of BFDV strains based on whole genome sequences. The tree was constructed using the neighbor-joining method in MEGA v5.2 with 1000 bootstrap replications. The FZ strain was signed with red dot. **A** Phylogenetic analysis of whole-genome sequences of FZ strain and 43 previously published BFDV strains. **B** Phylogenetic analysis of the *Rep* gene in 42 strains of BFDV. **C** Phylogenetic analysis of *Cap* gene in 24 strains of BFDV.

using anti-GST mouse monoclonal antibody revealed the presence of a distinct band of approximately 50 kDa, further confirming the expression of GST-cap in *E. coli* (Fig. 5E). Subsequently, polyclonal anti-Cap antibody was prepared in rabbits. Western blotting analysis showed that a dilution of the serum obtained from rabbits could detect the

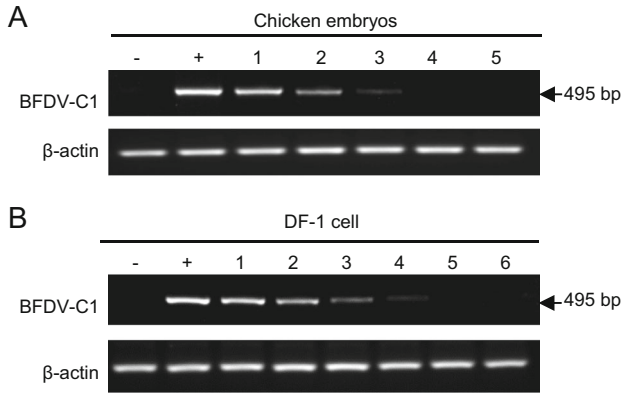

Fig. 4 BFDV replication in SPF chicken embryos and DF-1 cells. **A** The supernatant of BFDV-positive liver homogenate was used to infect SPF chicken embryos and blindly passaged for five generations for virus detection by PCR. **B** The supernatant of BFDV-positive liver homogenate was used to infect DF-1 cells and blindly passaged for six generations for virus detection by PCR. Lane 1–6, different blindly passages.

Cap protein of BFDV in the liver lysates of infected parrots but not in those of healthy (control) parrots (Fig. 5F).

Discussion

In this study, diseased parrots displayed the typical clinical symptoms of BFDV, including feather loss and beak deformation. Pathological sections of diseased parrots showed edema and necrosis of liver tissue and edema of renal tubular epithelial cells. These results are similar to those previously reported (Schoemaker *et al.* 2000). Previously, BFDV was reported to be co-infected with APV in psittacine birds, with a total infection rate of 10.33% (Hsu *et al.* 2006). The clinical and pathological signs of avian polyoma caused by APV are similar to those caused by BFDV. In our study, all samples have been tested and were negative for APV. The results of PCR amplification and

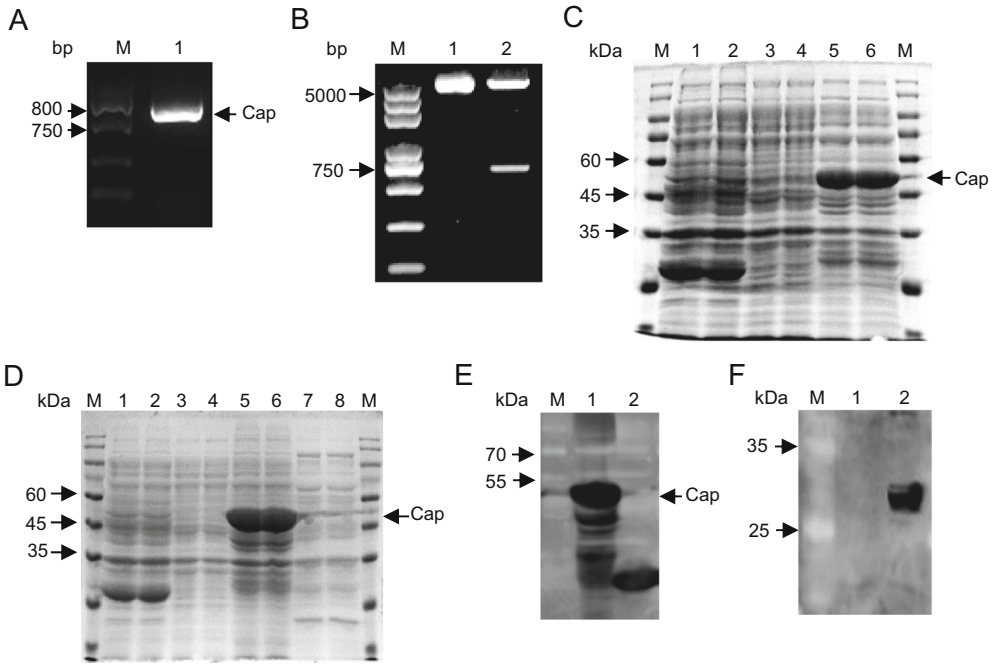

Fig. 5 Preparation of polyclonal anti-Cap antibody and examination of BFDV Cap protein in infected parrots. **A** Gel electrophoresis of the target *Cap* gene amplified by PCR. Lane 1, Cap gene product; Lane M, DNA marker. **B** Identification of the recombinant plasmid pGEX-4T-1-Cap using restriction endonucleases. Lane 1, recombinant plasmid pGEX-4T-1-Cap; Lane 2, recombinant plasmid pGEX-4T-1-Cap digested with *Xho* I and *Bam*H I; Lane M, DNA marker. **C** Bacterial lysates of E. coli BL21 Star (DE3) cells containing pGEX-4T-1 or recombinant plasmid analyzed by SDS-PAGE. Lanes 1 and 2, bacterial lysates of cells containing pGEX-4T-1; Lanes 3 and 4, bacterial lysates of cells containing pGEX-4T-1-Cap before induction; Lanes 5 and 6, bacterial lysates of cells containing pGEX-4T-1-Cap after induction with IPTG. Lane M, protein marker. **D** Analysis of the solubility of the GST-Cap fusion protein by SDS-PAGE. Lanes 1 and 2, bacterial lysates of cells containing pGEX-4T-1; Lanes 3 and 4, bacterial lysates of cells containing pGEX-4T-1-Cap before induction; Lanes 5 and 6, insoluble fraction of bacterial lysates of cells harboring pGEX-4T-1-Cap after induction with IPTG; Lanes 7 and 8, soluble fraction of bacterial lysates of cells harboring pGEX-4T-1-Cap after induction with IPTG. Lane M, protein marker. **E** Analysis of the GST-Cap fusion protein by Western blotting with GST antibody. Lane 1, expression of GST-Cap fusion protein after induction with IPTG; Lane 2, expression of GST protein after induction with IPTG; Lane M, protein marker. **F** Identification of Cap protein in liver samples of parrots by Western blotting with polyclonal anti-Cap antibody. Lane 1, BFDV-negative protein sample of liver. Lane 2, BFDV-positive liver sample. Lane M, protein marker.

DNA sequencing indicated that these parrots were infected with BFDV. Together, clinical signs and pathological changes in infected parrots suggest that the BFDV FZ strain is pathogenic in lorikeets.

Whole genome sequencing revealed that the length of the BFDV FZ strain genome is 1,995 bp, which is consistent with the previously reported genome size of BFDV (Sarker *et al.* 2015b). BLAST searches and bioinformatics analysis revealed that the FZ strain and New Caledonia strains were located on the same evolutionary branch, indicating that the FZ strain is the most closely related to these strains. This finding suggests a possible origin given the available dataset. Because the parrots are captive, it is likely in this instance that infected individual(s) was introduced to the captive flock without correct quarantine and biosecurity protocols. These results show that international control of on cross-boundary spread of animal infectious diseases is very important. Comparison between the FZ strain and strains of New Caledonia revealed a total of 123 nucleotides changed, among which two were insertions and three were deletions in the FZ strain. These data indicate that the FZ strain may have evolved, leading to the increased pathogenicity. Additionally, the whole-genome sequence of the FZ strain showed high genetic homology (80.0%–92.0%) with other 43 BFDV strains.

Previously, infectious clones of the goose circovirus (GoCV) have been used for the inoculation of goslings and goose embryos to generate an anti-GoCV antibody for detecting the replication of GoCV *in vivo* (Xu *et al.* 2012). In this study, we employed several methods to propagate the FZ strain of BFDV *in vitro*, such as SPF chicken embryos and the DF-1 cell line. The BFDV genes were detected in chicken embryos by PCR in the first several passages, but were undetectable after four passages. Similarly, BFDV genes were detected in DF-1 cells in the first four passages but were undetectable in the fifth passage. These results indicate that BFDV can replicate *in vitro* for several generations, but its replication is limited. In view of this finding, it is difficult to further study the pathogenicity and pathogenesis of BFDV in experimental animals. According to the whole genome sequence of the FZ strain, the genes of interest could be cloned into a vector, and the resulting BFDV infectious clones could be used to inoculate parrot embryos or parrots. This represents a potentially effective method to study the pathogenicity of BFDV and remains an ongoing task.

The BFDV Cap protein is an important component of the viral particle responsible for infection. It induces the production of specific antibodies in the host, thus the examination of the anti-Cap antibodies using serological tests is an effective method for detecting BFDV. The Rep protein of BFDV plays an important role in the life cycle of the virus, as it is involved in DNA replication, protein expression, and the viral particle production. In this study, the recombinant fusion proteins, GST-Cap and GST-Rep, were successfully prepared by the expression of recombinant plasmids (data not shown for GST-Rep). We generated a polyclonal anti-Cap antibody, which was used to detect the Cap protein in infected parrots by Western blotting. These data suggested that the anti-Cap antibody may be further optimized and developed to detect BFDV infection in birds.

Acknowledgements This work was funded by the National Key Research and Development Program of China (2018YFD0500100, 2016YFD0500205), Discipline Development Grant from College of Animal Sciences FAFU(2018DK003), Natural Science Foundation of China (31602046), National Basic Research Program (973) of China (2015CB910502), Program for Fujian University Outstanding Youth Scientific Research, Science and Technology Innovation Special Foundation of Fujian Agriculture and Forestry University (KFA17229A), Collaborative Innovation Center of Animal Health and Food Safety Application Technology in Fujian, Fujian Vocational College of Agriculture (Kla17H01A).

Author Contributions YM, XC, and JLC conceived and designed the experiments. XC, KC, XZ, SY, and WC performed the experiments. YM, XC, KC, and XZ analyzed the data. YM and XC wrote the manuscript and prepared the Figures. YM, XC and SY checked and finalized the manuscript. YT and XC provided resources. All authors read and approved the final manuscript.

Compliance with Ethical Standards

Conflict of interest The authors declare that they have no conflicts of interest.

Animal and Human Rights Statement The animal protocol used in this study was approved by "the Regulation of College of Animal Sciences, Fujian Agriculture and Forestry University of Research Ethics Committee" (Permit Number PZCASFAFU2017006). All animal experiments were carried out according to the Regulations for the Administration of Affairs Concerning Experimental Animals approved by the State Council of People's Republic of China.

References

Allan GM, Phenix KV, Todd D, Mcnulty MS (2010) Some biological and physico-chemical properties of porcine circovirus. Zentralbl Veterinarmed B 41:17–26

Amery-Gale J, Marenda MS, Owens J, Eden PA, Browning GF, Devlin JM (2017) A high prevalence of beak and feather disease virus in non-psittacine Australian birds. J Med Microbiol 66:1005–1013

Bassami MR, Berryman D, Wilcox GE, Raidal SR (1998) Psittacine beak and feather disease virus nucleotide sequence analysis and its relationship to porcine circovirus, plant circoviruses, and chicken anaemia virus. Virology 249:453–459

Bonne N, Shearer P, Sharp M, Clark P, Raidal S (2009) Assessment of recombinant beak and feather disease virus capsid protein as a vaccine for psittacine beak and feather disease. J Gen Virol 90:640–647

Crowther RA, Berriman JA, Curran WL, Allan GM, Todd D (2003) Comparison of the structures of three circoviruses: chicken anemia virus, porcine circovirus type 2, and beak and feather disease virus. J Virol 77:13036–13041

De KE, de Kloet SR (2004) Analysis of the beak and feather disease viral genome indicates the existence of several genotypes which have a complex psittacine host specificity. Adv Virol 149:2393–2412

Feng R, Wang X, Li J, Chen K, Guo G, Liao Y, Sun L, Huang S, Chen JL (2018) Interaction of Abl tyrosine kinases with SOCS3 impairs its suppressor function in tumorigenesis. Neoplasia 20:1095–1105

Finsterbusch T, Steinfeldt T, Caliskan R, Mankertz A (2005) Analysis of the subcellular localization of the proteins Rep, Rep' and Cap of porcine circovirus type 1. Virology 343:36–46

Fogell DJ, Martin RO, Groombridge JJ (2016) Beak and feather disease virus in wild and captive parrots: an analysis of geographic and taxonomic distribution and methodological trends. Arch Virol 161:2059–2074

Fogell DJ, Martin RO, Bunbury N, Lawson B, Sells J, McKeand AM, Tatayah V, Trung CT, Groombridge JJ (2018) Trade and conservation implications of new beak and feather disease virus detection in native and introduced parrots. Conserv Biol 32:1325–1335

Guo X, Ge X, Chang J (2018) Complete genome sequence of beak and feather disease virus isolated from an African grey parrot in China in 2017. Genome Announc 6:e01517–e01519

Heath L, Williamson AL, Rybicki EP (2006) The Capsid protein of beak and feather disease virus binds to the viral DNA and is responsible for transporting the replication-associated protein into the nucleus. J Virol 80:7219

Hsu CM, Ko CY, Tsai HJ (2006) Detection and sequence analysis of avian polyomavirus and psittacine beak and feather disease virus from psittacine birds in Taiwan. Avian Dis 50:348–353

Ignjatovic J (2010) Circoviridae: new viruses of pigs, parrots and chickens. Aust Vet J 72:40

Jergens AE, Brown TP, England TL (1988) Psittacine beak and feather disease syndrome in a cockatoo. J Am Vet Med Assoc 193:1292–1294

Kou Z, Zhang Z, Chen S, Fan Z, Tang S, Zhao L, Li T (2008) Molecular characterizations of avian polyomavirus isolated from budgerigar in China. Avian Dis 52:451–454

Lee B, Hyatt AD, Veronica O, Hengstberger SG, Donna B, Gerry M, Kaye H, Longcore JE (2002) Production of polyclonal antibodies to *Batrachochytrium dendrobatidis* and their use in an immunoperoxidase test for chytridiomycosis in amphibians. Dis Aquat Org 48:213

Mcorist S, Black DG, Pass DA, Scott PC, Marshall J (1984) Beak and feather dystrophy in wild sulphur-crested cockatoos (cacatua galerita). J Wildl Dis 20:120

Nagase C, Goryo M, Okada K (2005) Histopathological study of cockatiels inoculated with the psittacine beak and feather disease virus. J Jpn Vet Med Assoc 58:547–550

Niagro FD, Forsthoefel AN, Lawther RP, Kamalanathan L, Ritchie BW, Latimer KS, Lukert PD (1998) Beak and feather disease virus and porcine circovirus genomes: intermediates between the geminiviruses and plant circoviruses. Adv Virol 143:1723–1744

Pass DA, Perry RA (1984) The pathology of psittacine beak and feather disease. Aust Vet J 61:69–74

Raidal SR, Cross GM (1994) Control by vaccination of psittacine beak and feather disease in a mixed flock of Agapornis spp. Aust Vet Pract 24:178–180

Raidal SR, Firth GA, Cross GM (1993) Vaccination and challenge studies with psittacine beak and feather disease virus. Aust Vet J 70:437

Regnard GL, Rybicki EP, Hitzeroth II (2017) Recombinant expression of beak and feather disease virus capsid protein and assembly of virus-like particles in *Nicotiana benthamiana*. Virol J 14:174

Ritchie BW, Niagro FD, Lukert PD, Latimer KS, Steffens WL, Pritchard N (1989a) A Review of psittacine beak and feather disease: characteristics of the PBFD virus. J Assoc Avian Vet 3:143–149

Ritchie BW, Niagro FD, Lukert PD, Rd SW, Latimer KS (1989b) Characterization of a new virus from cockatoos with psittacine beak and feather disease. Virology 171:83–88

Sarker S, Ghorashi SA, Swarbrick CM, Khandokar YB, Himiari Z, Forwood JK, Raidal SR (2015a) An efficient approach for recombinant expression and purification of the viral capsid protein from beak and feather disease virus (BFDV) in *Escherichia coli*. J Virol Methods 215–216:1–8

Sarker S, Moylan KG, Ghorashi SA, Forwood JK, Peters A, Raidal SR (2015b) Evidence of a deep viral host switch event with beak and feather disease virus infection in rainbow bee-eaters (merops ornatus). Sci Rep 5:14511

Sarker S, Lloyd C, Forwood J, Raidal SR (2016) Forensic genetic evidence of beak and feather disease virus infection in a powerful owl, ninox strenua. Emu Austral Ornithol 116:71–74

Schoemaker NJ, Dorrestein GM, Latimer KS, Lumeij JT, Kik MJ, Van MDH, Campagnoli RP (2000) Severe leukopenia and liver necrosis in young African grey parrots (psittacus erithacus erithacus) infected with psittacine circovirus. Avian Dis 44:470–478

Subir S, Terrón MC, Yogesh K, David A, Hardy JM, Mazdak R, Manuel JZ, De PPJ, Fasséli C, Daniel L (2016) Structural insights into the assembly and regulation of distinct viral capsid complexes. Nat Commun 7:13014

Todd D (2004) Avian circovirus diseases: lessons for the study of PMWS. Vet Microbiol 98:169

Wang S, Zhang L, Zhang R, Chi X, Yang Z, Xie Y, Shu S, Liao Y, Chen JL (2018) Identification of two residues within the NS1 of H7N9 influenza a virus that critically affect the protein stability and function. Vet Res 49:98

Woods LW, Latimer KS (2000) Circovirus infection of nonpsittacine birds. J Avian Med Surg 14:154–163

Xu YP, Tian J, Yuan HX, Guo J, Sun HX, Li WW, Chen WH, Yu XP (2012) Construction and transfection experiment of a goose circovirus infectious clone. Chin J Virol 28:29–34

Yang J, Wang J, Chen K, Guo G, Xi R, Rothman PB, Whitten D, Zhang L, Huang S, Chen JL (2013) eIF4B phosphorylation by pim kinases plays a critical role in cellular transformation by Abl oncogenes. Cancer Res 73:4898–4908

Zhuang Q, Chen J, Mushtaq MH, Chen J, Liu S, Hou G, Li J, Huang B, Jiang W (2012) Prevalence and genetic characterization of avian polyomavirus and psittacine beak and feather disease virus isolated from budgerigars in Mainland China. Adv Virol 157:53–61